79 GHz LTCC-Integrated Antennas

Frank Bauer[(1)], **Wolfgang Menzel**[(2)]

(1) Institute of Microwave Techniques, University of Ulm, D-89069 Ulm, Germany
Email: frank.bauer@uni-ulm.de

(2) Institute of Microwave Techniques, University of Ulm, D-89069 Ulm, Germany
Email: wolfgang.menzel@uni-ulm.de

ABSTRACT: LTCC has proven to be an excellent technology for high density integration of passive multilayer circuits; frequency of operation has been continuously increased and now is reaching the higher mm-wave range, for example for automotive radar sensor applications. This contribution presents design approaches for planar antennas in the 76 GHz to 81 GHz frequency range – a slotted synthetic waveguide antenna and a grid antenna array. Four chains of a grid antenna then are integrated on a single LTTC substrate with a SiGe four-channel radar MMIC to form a short-range automotive sensor (with a range of a few tens of meters).

INTRODUCTION

LTCC provides excellent possibilities for high density multilayer integration [1, 2]. Operating frequencies are increasing continuously; radar sensors at 24 GHz [3], front-ends at 60 GHz [4 - 7], and first antennas for the automotive frequency band (76 GHz – 81 GHz, [8]) have been reported. Very small structures with tight tolerance requirements can be realized on the outer sides of the LTCC stack using "fine line" or thin-film processes [9, 10]. Advantages for high frequencies are small via diameters and via spacings, challenges in antenna design are found due to the relatively high dielectric constant, accordingly, alternatives to patch antennas have been investigated like grid antennas [4, 7, 8]. As transmission lines, nearly all types of line may be realized in this techniques; attention has to be paid both to conductor as well as to dielectric loss; in particular, screen-printed lines within the LTCC stack may have rough edges or increased loss due to ceramic inclusions, and the dielectric loss depends on the material composition itself and the firing process. Furthermore, parallel-plate mode may be excited between metallization layers in different planes.

For the work described in the following, synthetic integrated waveguide (SIW) and fine-line microstrip-like structures on the LTCC surface were employed; a number of tests have been performed with different LTCC materials. As antenna structures, both slotted waveguide arrays as well as grid antennas have been realized. Due to the multilayer structure of LTCC, feeding was partly done from the backside including the necessary transitions. This also enables to place active circuits on the backside without enlarging the overall circuit size.

SYNTHETIC INTEGRATED WAVEGUIDE

The general feeding network for the LTCC antennas is realized using synthetic integrated waveguide; top and bottom wall are standard metallization layer, while the sidewalls are realized by rows of vias with 0.1 mm diameter and spacings of 0.3 mm. Different types of LTCC materials have been considered in the first step, but although a material from Dupont (DuPont 943) shows very low-loss ($\tan\delta = 0.002 \ldots 0.003$, $\varepsilon_r \approx 7.4$), it is not suitable for a fine line process as required for 79 GHz. This is possible by a TDK material (TDK S39F), this however exhibits a loss tangent of about 0.008; some improvement is possible by extended firing ($\tan\delta = 0.006$, $\varepsilon_r \approx 7.3$). Just recently, an improved material is announced with a loss tangent of 0.003. Tests with an SIW of 0.55 mm height and 1.25 mm widths (loss tangent 0.006) show a loss of 0.5 … 0.6 dB/cm.

For measurement access to all antennas, a transition from SIW to standard waveguide according to Fig. 1 has been designed and optimized. It includes an opening on the substrate surface; with holes around the transition for screws and dowel pins, a standard waveguide flange can be connected. This transition exhibits a 10 GHz bandwidth (at 10 dB return loss). Measured insertion loss of a back-to-back configuration, connected by a 22.25 mm long section of SIW, results in an insertion loss of 2.4 dB (Fig. 1).

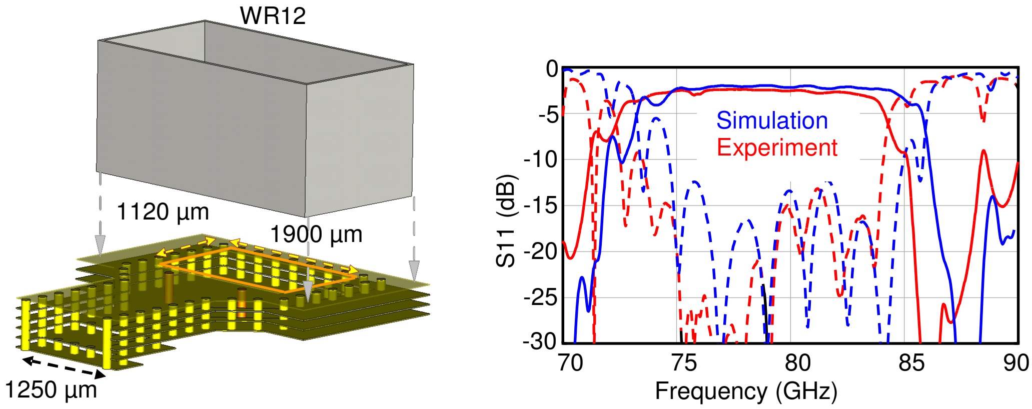

Fig. 1: Basic structure of a transition from SIW to standard waveguide and performance of a back-to-back configuration of two such transitions with 22.25 mm of SIW in between.

LTCC ANTENNAS

1. Slotted SIW Array

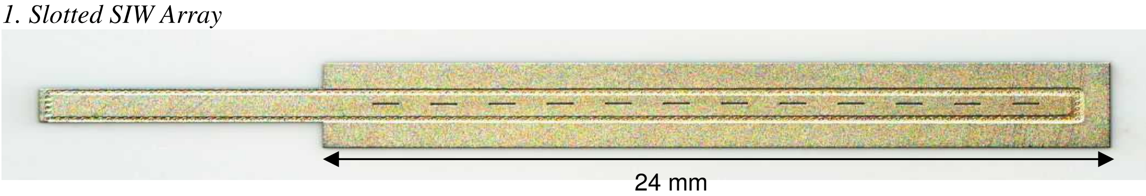

Fig. 2: Photograph of one row of an SIW slotted array.

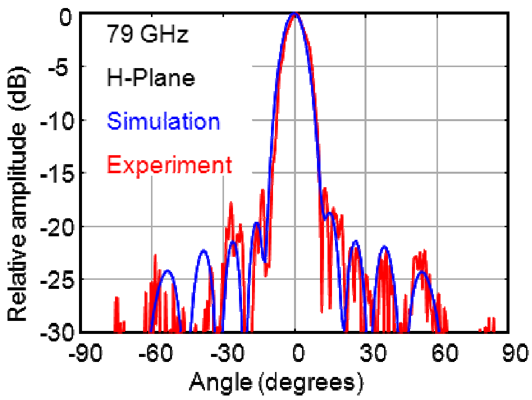

Fig. 3: H-plane radiation diagram of one row of an SIW slotted array.

A direct use of SIW for an antenna is the inclusion of slots into the upper metallization. According to the high dielectric constant and therefore relatively short guided wavelength, slots were placed only on one side (Fig. 2), avoiding, at the same time, a too close spacing and therefore coupling of the single slots. Except for the dielectric constant, standard procedures can be used for the design ([12]). One challenge are the small offset and small width of the slots, resulting in tight tolerance requirements, but feasible with the fine line technique. The H-plane radiation diagram of a single row is plotted in Fig. 3, showing an excellent agreement with a full wave simulation of the complete row and experiment. Beamwidth is about 12° in this plane. In the orthogonal direction, a very wide beamwidth results from the small dimensions in this plane. In principle, several such rows can be arranged side by side, together with an SIW power divider.

2. Grid Antenna

The first version of a grid antenna has been presented already in 1964 [11]. It consists of some kind of double meander microstrip structure as depicted in Fig. 4. All segments are about half a guided wavelength long; the currents in the longitudinal direction have the same direction and contribute in-phase to a broadside radiation. As there are no strong resonances, this type of antenna is more broadband, even for high dielectric constants, and less sensitive to tolerances.
Several segments can be put together; feeding can be done at one end or at suitable positions within the chain. In the design as used here, probe-type transitions to an SIW below the grid antenna are used (see Fig. 4, right side). Two antenna chains are placed back to back to compensate for a frequency dependent beam squint. Another layer of SIW feeds the middle SIW and connects the antenna either to the active circuit or to a waveguide transition for testing (Fig. 5).

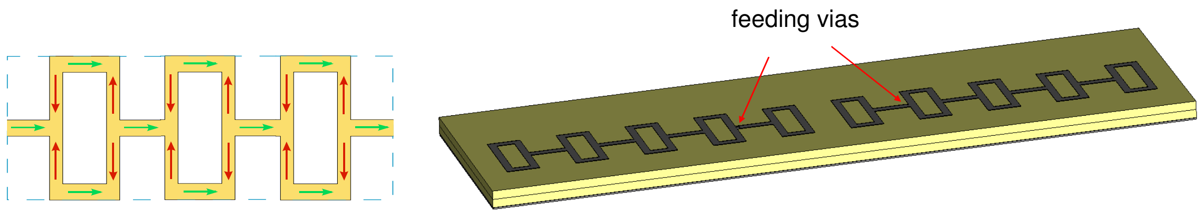

Fig. 4: Principle structure of a grid antenna.

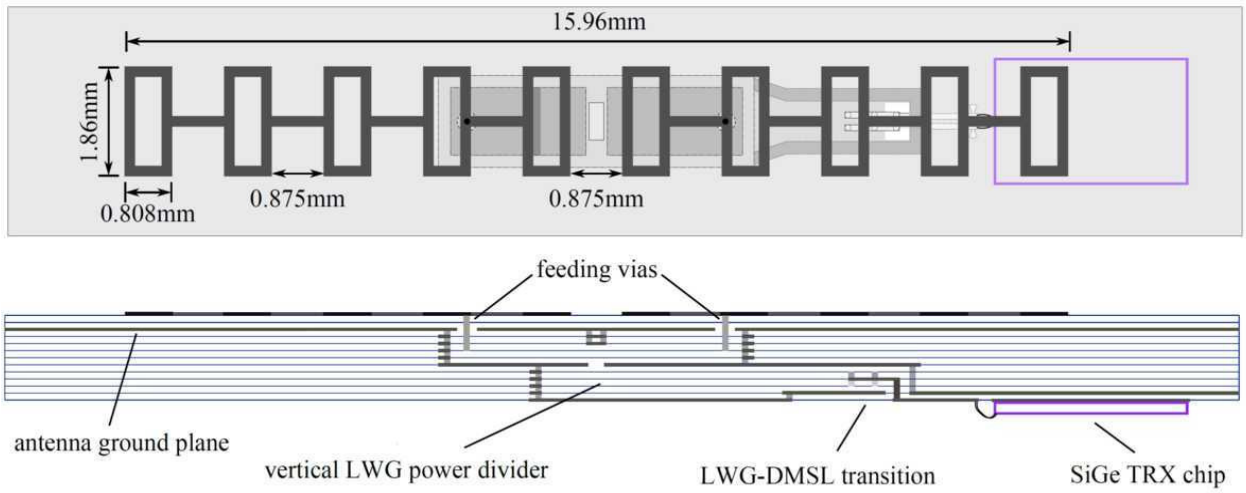

Fig. 5: View onto and cross section of the overall grid antenna configuration.

A single antenna chain has been fabricated (including a waveguide transition) and tested. Unfortunately, the thickness of the ceramic layers came out with 135 µm instead of 118 µm, so the waveguide transition did no longer work properly, but the antenna itself still worked. The antenna was re-calculated for the actual layer thickness, and reflection measurements were done using time gating. The results for both reflection coefficient and radiation diagrams are shown in Fig. 6, showing a satisfying agreement between simulation and experiment.

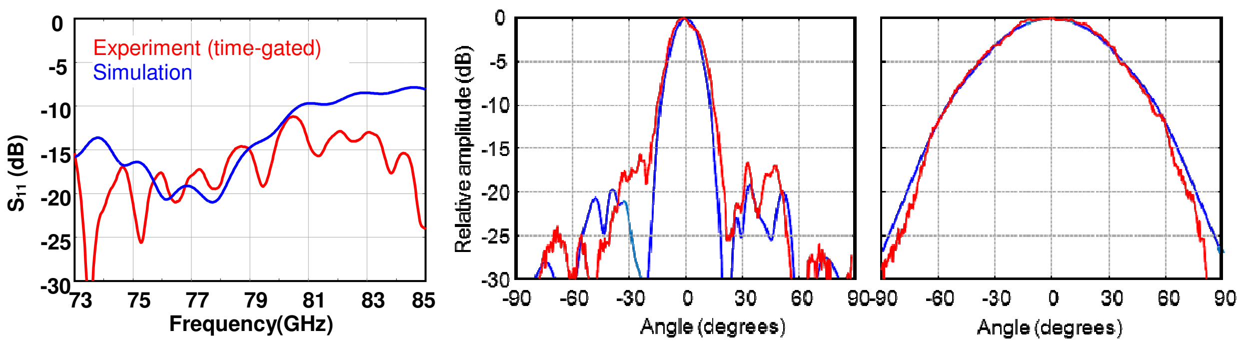

Fig. 6: Reflection coefficient and radiation diagrams of the grid antenna according to Fig. 5 (center: E-plane, right: H-plane, blue: simulation, red: experiment).

RADAR SENSOR WITH BEAMFORMING ANTENNA

Two grid antennas as shown in Fig. 5 and two similar antennas composed of a double chain then have been integrated on a one by one inch LTCC substrate. The lower SIW feed guides of each chain then are equipped with a transition to a symmetrical parallel strips on the back bonded to a SiGe four channel radar MMIC (Fig. 5, Fig. 7, [13]) on the same side. For a non-ambiguous beamforming process, at least two of the antenna chains have to be arranged together as close to half a wavelength as possible, so two single chains are placed in the centre. The two double chains provide an improved gain and are placed at different distances to allow both an increased overall aperture as well as a non-ambiguous superposition in beamforming. Test with that sensor exhibited a range of 15 m to 20 m for broadside direction and a lateral field of view of up to ±50° (with smaller range). As with this circuit, a substrate with a loss tangent of about 0.006 was used, losses in the feed network still are too high (and can be improved), and also the bond interconnect to the MMIC may be improved, so an increased range can be expected.

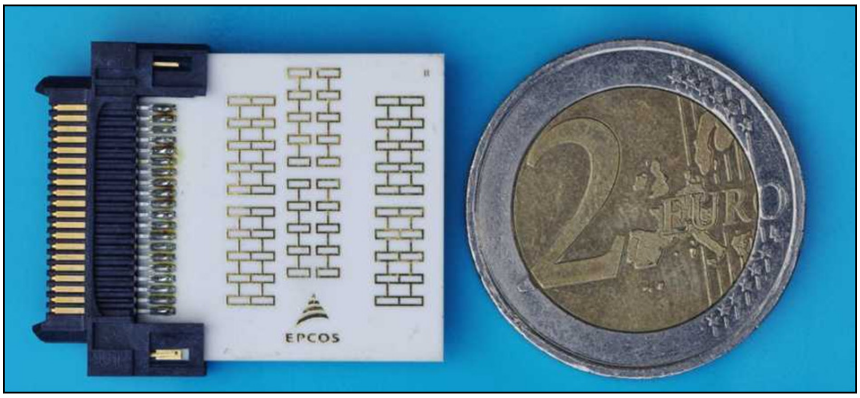

Fig. 7: Photograph of the LTTC circuit with four grid antenna chains, fed by SIW. A four-channel SiGe MMIC is integrated on the back side.

REFERENCES

[1] B. Geller et al., "LTCC-M: an enabling technology for high performance multilayer RF systems, *"IEEE MTT-S Symposium on Technologies for Wireless Applications (1999)*, pp. 189 - 192.

[2] R. Kulke, M. Rittweger, P. Uhlig, C. Günner, "Multilayer Ceramic For Wireless And Sensor Applications – LTCC," http://www.ltcc.de/downloads/rd/pub/10-doc-plus-engl-2001.pdf

[3] P. Uhlig, C. Günner, S. Holzwarth, R. Kulke, A. Lauer, M. Rittweger, "LTTC Short Range Radar Sensor for Automotive Applications at 24 GHz," *37th IMAPS, Long Beach, USA,* Nov. 2004, pp. 1 - 5.

[4] M. Sun; Y. P. Zhang; D. Liu; K. M. Chua; L. L. Wai, "A Ball Grid Array Package With a Microstrip Grid Array Antenna for a Single-Chip 60-GHz Receiver," *IEEE Transactions on Antennas and Propagation*, Vol. 59 , June 2011, pp. 2134 - 2140.

[5] R. Muller et al., "60 GHz ultrawideband hybrid-integrated dual-polarized front-end in LTCC technology", *5th European Conference on Antennas and Propagation (EUCAP 2011)*, pp. 1449 - 1453.

[6] J.-H. Lee, N. Kidera, G. DeJean, S. Pinel, J. Laskar, and M. M. Tentzeris, "AV-Band Front-End With 3-D Integrated Cavity Filters/Duplexers and Antenna in LTCC Technologies." *IEEE Trans. on Microwave Theory and Techniques*, Vol. 54, July 2006, pp. 2925 - 2936.

[7] L.L.Wai, K. M. Chua, A. C. W. Lu, Y. P. Zhang, M. Sun, "Ultra Compact LTCC Based AiP for 60 GHz Applications", *9th Electronics Packaging Technology Conference (EPTC 2007)*, pp. 595 - 599.

[8] F. Bauer, W. Menzel, "A 79 GHz Microstrip Grid Array Antenna Using a Laminated Waveguide Feed in LTCC," *IEEE AP-S/URSI Symposium 2011*, Spokane, pp. 2067 – 2070.

[9] J. Muller et al., "Technology Benchmarking of High Resolution Structures on LTCC for Microwave Circuits," *1st Electronics System Integration Technology Conference*, 2006, Vol. 1, pp. 111 - 117.

[10] S. Brunner, M. Stadler, X. Wang, F. Bauer, and K. Aichholzer, "Advanced high frequency LTCC technology for applications beyond 60 GHz," *8th International Conference on Ceramic Interconnect and Ceramic Microsystems Technologies (CICMT)*, Erfurt (Germany), Apr. 2012.

[11] J. Kraus, "A backward angle-fire array antenna," *IEEE Transactions on Antennas and Propagation*, vol.12, Jan 1964, pp. 48- 50.

[12] Shi Cheng, H. Yousef, H. Kratz, "79 GHz Slot Antennas Based on Substrate Integrated Waveguides (SIW) in a Flexible Printed Circuit Board," *IEEE Transactions on Antennas and Propagation*, vol.57, Jan. 2009, pp.64-71, Jan. 2009.

[13] C. Wagner, H.-P. Forstner, G. Haider, A. Stelzer, H. Jäger, "A 79-GHz Single-Chip Radar Transceiver with Switchable TX and LO Feedthru in a Silicon-Germanium Technology," *Proc. IEEE Bipolar / BiCMOS Circuits and Technology Meeting (BCTM2008)*, pp. 105-108, 13-15 Oct 2008.